OPTICAL PARAMETRIC DEVICES

A0005

Optical Parametric Oscillators (Continuous Wave)

S Schiller, Heinrich-Heine Universität Düsseldorf, Düsseldorf, Germany

S Schiller, Institut für Experimentalphysik, Heinrich-Heine-Universität Düsseldorf 40225 Düsseldorf, Germany

Key words: difference frequency generation; IR spectroscopy; mid-IR; nonlinear crystal; nonlinear frequency conversion; parametric fluorescence; parametric interaction; quasi-phasematching; spectroscopy; threshold; trace gas detection; twin beams; vibrational spectroscopy

S0005

Introduction

P0005 A continuous-wave optical parametric oscillator (cwOPO) is a frequency conversion device in which a continuous-wave (cw) laser field (pump) of frequency ω_p is partially converted into two cw waves of lower frequencies ω_s, ω_i (historically denoted by signal and idler) inside an optical cavity. The three frequencies are related by $\omega_i + \omega_s = \omega_p$. The cavity contains a nonlinear medium with a second-order susceptibility and the mirror reflectivities are chosen such that at least one of signal and idler resonates in the cavity. The conversion efficiency from pump power to signal or idler power or both can be larger than 10%. The frequencies of signal and idler waves can be tuned by means similar to conventional lasers, i.e., by changing the spectral dependence of the cavity loss and by tuning the cavity length. Additional tuning parameters specific to OPOs are the pump frequency and the refractive indices of the nonlinear medium for pump, signal and idler. CwOPOs provide a unique combination of features that makes them suitable sources for a variety of spectroscopic applications. Today's cwOPOs can exhibit the following features:

P0010 • spectral coverage from the near-infrared (0.7 μm) to the mid-infrared (5.2 μm); for a single device two optical octaves can be covered without change of optical components;

P0015 • high output power (up to several W);

P0020 • high pump power conversion efficiency (>30%) and good wall-plug efficiency;

P0025 • diffraction-limited (lowest order transverse electromagnetic mode of a laser (TEM_{00}) output beams;

P0030 • single-frequency output, absence of frequency jumps (mode hops);

P0035 • narrow free-running linewidth (<6 kHz);

P0040 • high absolute frequency stability (<100 MHz drift per hour);

P0045 • continuous frequency tuning exceeding 10 GHz;

P0050 • rapid, stepwise tuning over several THz; and

P0055 • transportability.

cwOPOs complement their pulsed relatives (*see* **Optical Parametric Devices:** Optical Parametric Oscillators (Pulsed) (00858)) nanosecond and synchronously pumped pulsed parametric oscillators (*see* **Optical Parametric Devices:** Overview (00757)).

S0010

Basic Principle

P0060 The operation of a cwOPO is most simply described for a singly-resonant OPO (SRO) (see **Figure 1** and **Figure 2a**).

P0065 Without loss of generality we take the signal wave to be the resonant wave. When a higher-frequency pump wave (power P_p, angular frequency ω_p) and a lower-frequency (signal) wave (power P_s, angular frequency ω_s) traverse a $\chi^{(2)}$ medium (*see* **Fiber and Guided Wave Optics:** Nonlinear Optics (00700)), a transfer of power from the pump wave to the signal

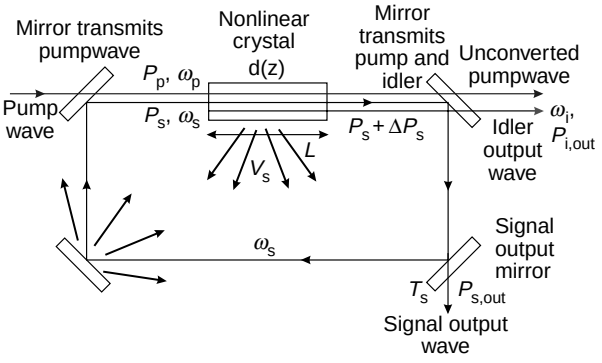

F0005 **Figure 1** Schematic of a singly-resonant cwOPO (SRO) in ring configuration. The signal wave (ω_s) is resonated, the idler wave (ω_i) is not. In the nonlinear crystal, the pump wave overlaps with the signal and idler waves; here they are shown displaced with respect to each other for clarity. The signal wave's loss coefficient per roundtrip, S_s, is the sum of loss inside the nonlinear crystal, V_s (indicated by arrows), and transmission through mirrors, here represented by a single mirror of transmission T_s. Scatter and absorption losses at mirrors (indicated by arrows) are included in V_s.

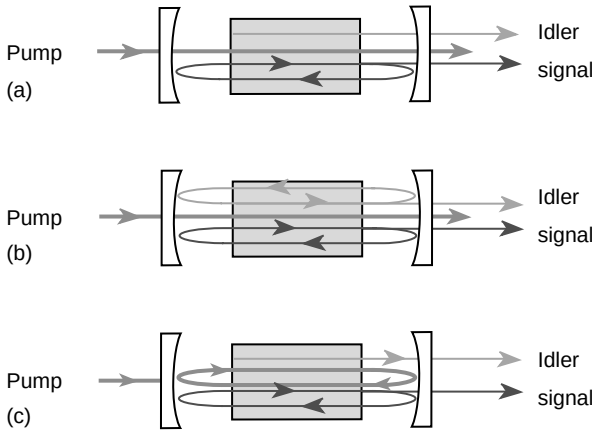

F0010 **Figure 2** Common types of cwOPOs. (a) basic SRO, (b) SRO with enhancement of the pump wave (PR-SRO); a common-cavity configuration is shown. (c) Doubly-resonant OPO (DRO). Standing-wave cavities are shown.

wave occurs, described by a power gain:

$$\Delta P_s = GP_s = EP_pP_s \qquad [1]$$

This parametric amplification expression is valid as long as $\Delta P_s \ll P_s, P_p$, i.e., in the limit of small gain and small pump depletion. The (unsaturated) gain coefficient E is a function of: the medium's index of refraction, orientation and length L, the frequencies ω_s, ω_p, and the spatial modes and overlap of the two beams.

P0070 If the wave ω_s is made to circulate inside a cavity and the power loss per roundtrip, S_sP_s is smaller than the power gain per roundtrip (eqn [1]), a sustained oscillation is possible. This is satisfied when the input pump power P_p exceeds the threshold:

$$P_{p,in}^{th} = S_s/E \qquad [2]$$

As the pump power P_p is increased above $P_{p,in}^{th}$, conversion of pump power to idler power occurs, implying that the pump power decreases within the medium. Qualitatively, the average pump power $\langle P_p \rangle$ along the medium remains at the level $P_{p,in}^{th}$, so that the roundtrip fractional power gain remains constant, $G \simeq E\langle P_p \rangle \simeq EP_p^{th} \simeq S_s$. This ensures that the device reaches a stationary state. The circulating signal power P_s increases steadily with increasing pump power, and so does the signal power emitted from the OPO, T_sP_s, which is equal to the 'useable' fraction of the roundtrip power gain, $(T_s/S_s)GP_s$.

P0075 The parametric process that allows the signal wave to experience gain (eqn [1]), also generates an idler wave (difference frequency generation). Its power at the end of the medium is given by the Manley–Rowe relation:

$$P_i = \frac{\omega_i}{\omega_s}\Delta P_s \qquad [3]$$

P0080 An OPO also requires a process that starts the oscillation. Spontaneous parametric fluorescence provides this trigger. Due to this quantum effect, a pump wave traversing a $\chi^{(2)}$ medium will generate a flux of signal photons even if there is no signal wave present at the crystal input face. In the photon picture, a tiny fraction (on the order 10^{-9} for a 1 W pump) of the pump photons spontaneously annihilate, creating pairs of signal and idler photons (photon splitting). The idler photons have a frequency $\omega i = \omega p - \omega s$, so that photon energy conservation holds. The process may be thought of as being stimulated by the vacuum fluctuations of the electromagnetic field at the signal and idler frequencies. Some of the signal photons are emitted into the cavity mode, so that after a roundtrip they can serve as a seed for further (stimulated) photon splitting. The process repeats, and the signal wave builds up exponentially in time to a macroscopic level if the pump power is above threshold. The spontaneous (as well as the parametric amplification) process is strongest when momentum conservation is essentially fulfilled, $k_p \simeq k_s + k_i$, where $k = \omega n(\omega)/c$.

P0085 In the photon picture, the relation (eqn [3]) is a statement that signal and idler photons are always created in pairs.

Types of OPOs

S0015

P0090 OPO types may be classified according to the number of waves that resonate within cavities. Typically, a realizable roundtrip loss coefficient is on the order of $S_s = 1\%$ (to which the linear absorption of the nonlinear crystal and mirror transmissivities contribute) and the gain coefficient $E \sim 0.1\%/\mathrm{W} - 1\%/\mathrm{W}$ for Gaussian waves, depending on the pump wavelength, crystal type, etc. This leads to SRO threshold powers on the order of 1 to 10 W. Until the early 1990s, solid-state pump lasers of this power level and single-frequency output were unavailable. This led to the interest in and development of cwOPOs in which more than one of the three waves is resonated (Figure 2). The corresponding external threshold powers are

$$P_{p,in}^{th} \simeq S_sS_i/4E \text{ for a doubly-resonant OPO (DRO, Figure 2b)}$$

$$P_{p,in}^{th} \simeq S_sS_p/E \text{ for a pump-resonant SRO (PR-SRO, Figure 2c, see eqn [3])}$$

$$P_{p,in}^{th} \simeq S_sS_iS_p/E \text{ for a triply-resonant OPO (TRO)} \qquad [4]$$

P0095 Typically, each additional resonant enhancement lowers the threshold power by one to two orders.

P0100 Examples for threshold values reported in the literature are: 1.9 W for a 920 nm-pumped SRO, 4 mW for a 0.5 μm-pumped DRO, and 140 mW for a 1 μm-pumped common-cavity PR-SRO. DROs can therefore be pumped even by low-power diode lasers. TROs (where pump, signal, and idler are resonated) are not of importance due to their higher complexity.

S0020

Output Power

P0105 As an example, the signal and idler output powers for a PR-SRO that resonates the signal are:

$$P_{s,out} \simeq T_s P_s(0), \qquad P_{i,out} \simeq (\omega_i/\omega_s) S_s P_s(0) \qquad [5]$$

where the circulating signal power is

$$P_s(0) \simeq \frac{\omega_s}{\omega_p} \frac{4T_p}{S_s S_p} P_{p,in}^{th} \left(\sqrt{\frac{P_{p,in}}{P_{p,in}^{th}}} - 1 \right) \qquad [6]$$

T_p is the input mirror transmission for the pump wave, and T_s is the output mirror transmission of the signal wave. Signal and idler output powers have the same dependence on pump input power and increase monotonically with $P_{p,in}$. The conversion efficiencies reach a maximum four times above threshold, i.e., when $P_{p,in} = 4P_{p,in}^{th}$. There, the signal and idler photon (quantum) conversion efficiencies $\omega_p P_{s,out}/P_{p,in}\omega_s$ and $\omega_p P_{i,out}/P_{p,in}\omega_i$ exceed 25% and 50%, respectively, if the mirror transmissions T_p, T_s for pump and signal are chosen larger than the respective roundtrip loss V_p, V_s. This can be achieved in practice, of course, at the expense of a higher threshold.

S0025

Nonlinear Materials

P0110 While the fundamental developments in cwOPOs were performed using birefringently phase-matched nonlinear crystals (MgO:$LiNbO_3$, LBO, KTP, $KNbO_3$) [**Reference Encyclop. Article on nonlinear crystals**], and substantial spectral coverage is possible with these crystals, most cwOPOs are now operated with quasi-phase-matched (QPM) nonlinear crystals [**Reference Encyclop. Article on phasematching**]. The most commonly used material is periodically poled (PP) $LiNbO_3$ (PPLN), other crystals used are PPKTP and PP$LiTaO_3$, crystals. Their use has led to a substantial widening of the spectral coverage, opening in particular the wavelength range $\lambda > 1.6$ μm, a reduction of the required pump powers thanks to their much higher nonlinearities compared to birefringently phase-matched crystals, and a simplification of (gross) tuning through the use of multigrating structures (containing several sections of differing Λ periods side by side within the same crystal). The above PP crystals exhibit a loss of 0.1%/cm at wavelength around 1 μm, and can be coated with broadband dielectric antireflection coatings, in order to maximize the overall transmission. Another important aspect is that the crystals withstand long irradiation times with high-power focused cw light. For PPLN, operation temperature above 100 °C is chosen in order to prevent photorefractive effects.

S0030

Spectral Coverage

P0115 An example of particularly wide spectral coverage reported in the literature is a cwOPO pumped by a frequency-doubled Nd:YVO_4 laser ($\lambda_p = 532$ nm) using a multigrating PPLN crystal. With grating periods $\Lambda = 6.5–9.6$ μm, the range 660–1030 nm (signal wave) and 1100–2800 nm (idler wave) was covered. A cwOPO with a Nd:YAG pump source emitting at the fundamental wavelength ($\lambda_p = 1064$ nm) and a multigrating PPLN crystal ($\Lambda = 25.5–31.2$ μm) achieved a range of 1.45–1.99 μm (signal) and 2.3–4.0 μm (idler).

P0120 For idler wavelengths beyond 4 μm, idler absorption by the crystals types above becomes relevant, leading to a reduction in the gain G (this effect is not considered in the treatment given in the Appendix) and to an increase of the threshold. To a certain extent, this can be compensated with powerful cw pump lasers. For example, a 1064 nm pumped PPLN-SRO achieved idler emission in the range 3.6–4.7 μm at 11 W pump power. Also, a 850 nm pumped PR-SRO covered an idler range 4.3–5.3 μm when pumped with 750 mW.

P0125 In the future, cwOPOs will certainly profit from the development of novel QPM materials with wider IR transparency range.

S0035

Frequency Control

P0130 The small-signal gain $G(\omega)$ of a parametric interaction in a cwOPO is analogous to the homogenously broadened gain in a laser medium. In contrast to it, however, spatial hole-burning cannot occur. Therefore, mode competition is generally strong in a cwOPO, which will oscillate on a single longitudinal mode: the one for which the difference (or ratio) between 'unsaturated' parametric gain G and total loss S is largest (**Figure 3**). This is equivalent to the condition of minimum threshold.

P0135 The functions $G(\omega)$ and $S(\omega)$ are therefore important characteristics of a cwOPO. Oscillation can only occur for a frequency ω that is very close to a cavity mode frequency $\omega_q = 2\pi qc/\mathrm{OPL}(\omega_q)$, where q is the

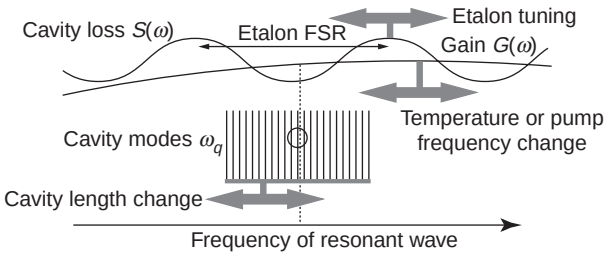

F0015 **Figure 3** Frequency selection and tuning in a SRO (with or without pump resonance) containing an etalon. Oscillation occurs on the signal cavity mode (circled) closest to the frequency where the difference between the small-signal gain G and the loss S is largest (dashed line). The frequency of this mode or the mode number q can be changed by changing the parameters indicated near the thick double arrows. Changing the temperature leads to a rough setting of the oscillation frequency. Tilting the etalon allows mode-hop tuning of signal and idler frequencies. Fine tuning by a small amount can be done by changing the cavity length. The frequency of the idler is not shown here; it is always given by the difference between pump frequency and the frequency of the oscillating mode. Thus, tuning of the pump frequency generally leads to a tuning of the idler frequency. For modest pump tuning the amount of signal tuning however depends on SRO type: no signal tuning in a basic SRO and in a dual-cavity PR-SRO, while in a common-cavity SRO pump and signal frequencies are correlated and thus pump tuning leads to signal tuning.

integer mode number, and the optical power limited OPL(ω) is the round-trip optical path length at the frequency ω.

P0140 To tune a cwOPO to a particular signal/idler frequency pair, a coarse tuning is initially performed by tuning the corresponding phase mismatch ΔkL (L is the crystal length) approximately to zero. Taking into account a modulation of the nonlinear susceptibility of the crystal with period Λ, the quantity $\Delta k = k_p - k_s - k_i \pm 2\pi/\Lambda$ describes the deviation from momentum conservation in the photon splitting process. When using a multigrating QPM crystal, the first tuning consists in the selection of a grating of appropriate period Λ, which is moved into the pump wavepath. This is followed by tuning the photon momenta via the refractive indices of the nonlinear medium, which is usually accomplished by temperature tuning, or alternatively by angle-tuning of the crystal. These steps place the maximum of $G(\omega)$ to the vicinity of the desired frequency. Options for tuning the emission exactly to the desired frequency are described below for the different OPO types.

P0145 Because external perturbations change parameters that enter in $G(\omega)$, $S(\omega)$, and ω_q, the value of the oscillating frequency will also change in time. The change will be continuous over a certain range of the parameters, but if their perturbation is large enough, a mode hop can occur: the oscillation on the initial mode q will eventually cease and another mode q', for which $G(\omega_{q'}) - S(\omega_{q'})$ is larger, will oscillate instead. A variety of parameters is affected by perturbations: pump power, pump beam direction, cavity length, crystal temperature, and pump frequency.

P0150 When such perturbations are applied on intentionally, the OPO output frequencies can be tuned, scanned, or adjusted. The tolerable change in the various parameters before a mode-hop occurs, and the sensitivity of the output frequencies to changes in the parameters depends on the particular cwOPO type. One important approach to suppress mode-hops consists in adding elements into the cavity, such as an etalon, that modify the function $S(\omega)$, typically by modulating it spectrally.

SRO

S0040

P0155 In the following, we assume that the signal wave is resonated. The SRO is the simplest cwOPO type. The oscillation nominally occurs at the cavity frequency that is closest to the gain maximum, as described above. In practice, environmental disturbances will cause mode-hops on a time-scale of minutes. For this reason, an etalon is added to the cavity. Mode-hop-free oscillation, for several hours, is then achieved.

P0160 Typical nonlinear crystals exhibit parametric gain with spectral widths of hundreds of GHz. In contrast, the cavity mode spacing (free spectral range) c/OPL is on the order of 1 GHz. The tuning range achievable by a cavity length change (using e.g., a piezo translator) is therefore, at most, one free spectral range (equal but opposite for signal and idler); then a mode-hop to the neighboring cavity mode occurs, with a signal/idler frequency jump by one FSR in the Q1 opposite direction to the previous tuning. This process repeats itself as the cavity length is tuned further. It is, therefore, not possible to easily and reliably access a large frequency range by using the cavity length as tuning parameter.

P0165 As shown in Figure 3, if an etalon of linewidth smaller than the gain bandwidth is added to the cavity, it becomes the dominant influence (etalon FSRs on the order of one hundred to a few hundred GHz have been used). This means that shifting the etalon's transmission maximum (i.e., the cavity loss S) in frequency space (by tilting a solid etalon or changing the spacing of an air-spaced etalon) as indicated by the double-headed arrow in Figure 3, forces the signal to mode-hop to an adjacent mode, with a corresponding idler frequency hop in the opposite direction. As the etalon is tuned further this occurs repeatedly. This discontinuous 'mode-hop tuning' is useful for tuning the SRO output frequencies over a significant range (e.g., 100 GHz) and

allows to reach a desired frequency within one cavity free spectral range.

P0170 Continuous tuning of both signal and idler waves is obtainable, if the pump laser is not frequency tunable, by changing the cavity length and synchronously tuning the etalon. This can be achieved by a feedback or feedforward system that controls the etalon angle or spacing. Up to 38 GHz tuning for signal and idler were achieved in this way.

P0175 When a tuneable pump is available, one can tune the pump frequency while keeping the cavity length and the etalon angle fixed. This keeps the signal cavity mode fixed, and thus the nonresonant wave's frequency (usually the idler) is tuned by an amount equal to the pump frequency change. Continuous tuning ranges exceeding 50 GHz have been obtained in this way. For such pump tuning ranges, the shift of the gain curve, indicated by a double-arrow in Figure 3, is usually sufficiently small that it can be neglected. The use of a widely tuneable pump laser is also possible. A (discontinuous) idler tuning of 9 THz around 3.3 μm has been demonstrated, covered in just 0.3 ms thanks to a large pump tuning rate. In such a case of large pump tuning range, the gain shift is important causing a significant tuning also of the signal.

P0180 The advantages of the basic SRO as compared to other cwOPOs are mainly the simpler tuning behavior, the possibility of continuous tuning without necessitating a tunable pump laser, and the possibility to achieve a very wide tuning range without optics change, since only the spectral range covered by one of the two parametric waves must be provided as a high reflectivity coating on the cavity mirrors. Moreover, in the simplest implementation, it is possible to operate without any electronic servo control of cavity elements, at the expense of a reduced power and frequency stability. In terms of spectral properties (linewidth, frequency stability, time between undesired mode-hops) the SRO does not offer particular advantages compared to other cwOPO types, even if actively stabilized (see below). The disadvantage of the basic SROs based on Gaussian modes is the high threshold, necessitating expensive high-power (several W) cw lasers. This disadvantage is likely to disappear with progress in laser development. The alternative of waveguide SROs is mentioned below.

S0045 PR-SRO

P0185 In a PR-SRO, the pump wave is also resonated, leading to a substantial reduction of threshold. For example, it is possible to generate mid-IR radiation (3 μm range), even with much more affordable 1 W-level Nd:YAG pump lasers.

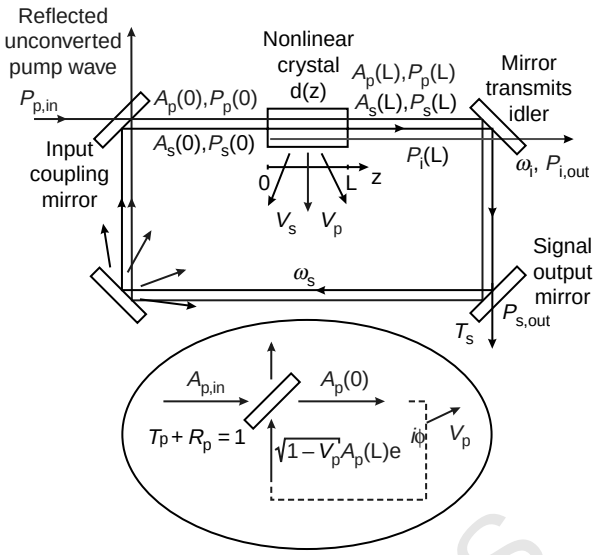

Figure 4 Schematic of a pump-resonant SRO with a common cavity for pump and signal waves. The inset shows the pump wave fields incident on and leaving the input coupling mirror. F0020

One implementation is the common-cavity PR-SRO (Figure 4). The cavity length is either locked to the pump laser frequency or vice-versa. If a frequency-stable pump laser is used, the first solution is favorable, since then both signal and idler waves have a stability comparable to that of the pump laser. With an etalon (coated so as to be transparent for the pump wave) inside the cavity, mode-hop-free operation for several hours has been demonstrated. P0190

Mode-hop tuning in a PR-SRO with cavity-to-laser lock can be achieved: P0195

(i) by tuning the etalon at constant pump frequency: the signal mode-hops from mode to mode, the idler tunes equally but in opposite direction; P0200

(ii) by tuning the pump frequency at constant etalon position: the cavity length must follow and therefore the signal tunes by $\Delta\omega_s = (\omega_s/\omega_p)\Delta\omega_p$, while the idler frequency tunes by $\Delta\omega_i = (\omega_i/\omega_p)\Delta\omega_p$. This continues until the signal must mode-hop back, causing an equal but opposite frequency jump in the idler. The pump tuning is thus completely transferred to the idler. P0205

Continuous signal and idler tuning is performed by tuning the pump frequency and synchronously adjusting the etalon angle. Thus, a limitation of the common-cavity PR-SRO concept is that continuous tunability necessitates a tunable pump laser. P0210

In a dual-cavity, PR-SRO pump and signal wave resonate in separate cavities. The pump cavity is usually stabilized to the pump frequency and an P0215

etalon is placed into the signal cavity for better stability against mode-hops. This configuration combines the tuning simplicity of a basic SRO with a low threshold power. For example, a threshold for a 1 μm-pumped PPLN dual-cavity PR-SRO at the 0.4 W level was obtained.

P0220 Mode-hop tuning (in opposite directions) of the frequencies of both parametric waves in steps of the cavity's FSR can be performed by changing the etalon angle (Figure 3). A range exceeding 50 GHz (at constant output power) has been achieved. Continuous signal and idler wave tuning (by equal but opposite amounts) is possible by changing the signal cavity length (Figure 3). However, the range is limited to the FSR of the cavity, typically on the order of 500 MHz, then the frequencies mode-hop back. It is expected that wider continuous tuning should be possible by synchronous etalon and cavity length scan. If a tuneable pump laser is employed, continuous tuning of only the idler frequency is possible by keeping the etalon and signal wave cavity length fixed; the pump tuning range is fully transferred to the idler.

S0050 DRO

P0225 In contrast to an SRO, this device type requires both parametrically generated waves to be resonant in the cavity. Here we consider only DROs with a common cavity for both signal and idler waves (dual-cavity DROs have also been demonstrated).

P0230 Because of the added resonance condition, mode-hops of the oscillating mode pair occur already upon a very small change (~1 nm) in the cavity length. Under normal environmental conditions such changes are unavoidable and therefore a 'free-running' DRO does not produce frequency-stable output. However, by active control of one additional parameter of the OPO system the mode-hops can be effectively suppressed. A practical solution is to actively control the length of the cavity via the position d of one of the cavity mirrors so that a particular mode pair, q_s, q_i, continues to oscillate; this is achieved by maximizing the OPO output power or by minimizing the detuning of one of the two resonant waves from its respective cavity mode frequency. This control system ensures that energy conservation and the two resonance conditions are simultaneously satisfied:

$$\begin{aligned} \omega_s + \omega_i &= \omega_p \\ \omega_s &= 2\pi c q_s/\mathrm{OPL}(d, \omega_s, T) \\ \omega_i &= 2\pi c q_i/\mathrm{OPL}(d, \omega_i, T) \end{aligned} \quad [7]$$

Q7

Experimentally, mode-hop-free oscillation exceeding 10 h was achieved by such active stabilization.

P0235 Another system parameter may then be used to tune both signal and idler frequencies. The tuning coefficient for the crystal temperature T is small, but tuning the pump frequency is an efficient way. The tuning coefficient is approximately $\Delta\omega_s = (\omega_s/\omega_p)\Delta\omega_p$, and accordingly for ω_i.

P0240 Continuous tuning of signal and idler frequencies over 10 GHz by pump tuning was achieved. This range was limited by the available continuous tuning range of the pump laser. Mode-hop tuning can be induced by mechanical perturbations: by tapping on the DRO cavity, mode-hop tuning over 220 GHz has been demonstrated.

Linewidth and Frequency Stability S0055

P0245 For high-resolution spectroscopy a narrow linewidth for signal or idler is desirable. One contribution to the linewidth of a cwOPO arises from the unavoidable spontaneous parametric fluorescence, similar to the Schawlow–Townes limit in lasers due to spontaneous emission. This contribution is negligible if the OPO operates at power levels of practical interest. Thus, other sources of classical noise dominate the linewidth of cwOPOs. As discussed above, the frequency of cwOPOs depends (on a fine scale) on pump frequency and cavity optical path length. Both parameters fluctuate: the pump laser has a finite linewidth as well as frequency jitter, and the cavity optical path length fluctuates due to acoustic noise affecting the mirror positions, to air pressure fluctuations, temperature fluctuations of the crystal and of the cavity structure.

P0250 With careful construction and shielding, many of these noise sources can be minimized. Furthermore, it is highly favorable to use pump lasers of narrow linewidth and high intrinsic frequency stability (e.g., diode-pumped monolithic solid-state lasers), or actively frequency stabilized lasers. Note that this special requirement on the pump source does not exist for lasers.

P0255 In an SRO, the linewidth and frequency stability of the signal are mostly determined by the stability properties of the cavity. The idler spectral properties then follow entirely from the signal and pump spectral properties through $\omega_i = \omega_p - \omega_s$. Since the idler is usually the wave of interest, this implies that the SRO cavity and the pump laser must both have a stability appropriate to the spectroscopic application.

P0260 If the SRO cavity is not sufficiently stable (e.g., because of insufficient temperature stability of the oven containing the nonlinear crystal), the frequency fluctuation/drift of the signal and idler

can be substantial, tens to hundreds of MHz within minutes being typical.

P0265 To avoid mode-hops also on long time-scales, the cavity length (or the etalon angle) can be actively stabilized so as to maximize the idler's output power. This ensures that the cavity mode position and the frequency of maximum difference between gain and loss are kept equal.

P0270 If a frequency-stable pump wave is used, it is possible to transfer these characteristics by stabilizing the SRO cavity length to the pump wave frequency. In an SRO without resonant pump one can make use of the residual reflection of the pump wave by the cavity mirrors that leads to interference with the pump wave reflected from the pump input mirror. This was implemented in a SRO pumped by a high-power diode-pumped internally doubled Nd:YVO_4 laser (532 nm) of high intrinsic frequency stability. Signal and idler drifts of less than 50-MHz/h were achieved. At the same time, a very small 20 kHz linewidth of the (resonant) signal radiation was obtained. Similar levels were obtained for a PR-SRO with a common cavity for pump and signal wave.

P0275 In a PR-SRO with dual-cavity configuration, the same requirements of minimization of disturbances to the parametric wave's cavity arise as in a basic SRO. Using a highly frequency-stable kHz linewidth monolithic pump laser, together with the above-mentioned idler power maximization control, frequency drift values for both parametric waves at the level of 30 MHz/h were obtained and a short-term linewidth below 6 kHz.

P0280 In a single-cavity DRO, the linewidth and frequency stability of the parametric waves are essentially determined by the pump wave properties (see discussion in the section on DRO above). Here, too, the use of narrow-linewidth, high frequency stability pump lasers has led to excellent signal/idler characteristics. For example, less than 40 kHz linewidth and <40 MHz per hour drift were obtained with a DRO pumped by an externally doubled monolithic Nd:YAG laser of 10 kHz linewidth.

P0285 If further narrowing of linewidth or reduction of frequency drift is desired, the OPO output frequencies can be stabilized to a stable cavity, atomic, or molecular transition. Locking to a cavity has been demonstrated for a DRO.

Applications

S0060

P0290 CwOPOs are most interesting as sources of radiation in the IR range beyond 2 μm, especially in the 3–5 μm range, where vibrational transitions of many molecules occur. In comparison to other sources of coherent radiation (color center laser, quantum cascade laser, lead-salt diode laser, CO overtone laser, difference frequency generation), cwOPOs provide a unique combination of desirable features.

P0295 A simple application of cwOPOs would be as a source providing a power level/output wavelength/-mode quality combination not available from other sources. Possible applications are vibrational spectroscopy in the condensed phase, where a narrow linewidth is not required. The excellent beam quality provides a high spatial resolution.

P0300 Concerning high-resolution spectroscopy (mostly in the gas phase), methods demonstrated in conjunction with cwOPOs include:

- P0305 Absorption spectroscopy;
- P0310 Doppler-free saturation spectroscopy;
- P0315 Photo-acoustic spectroscopy (PAS);
- P0320 Hole-burning spectroscopy;
- P0325 Coherent atomic spectroscopy;
- P0330 Cw cavity ring down spectroscopy (cw-CRDS).

P0335 Trace gas detection using PAS or cw-CRDS is a particular application where cwOPOs have reached excellent sensitivity (minimum detectable concentrations as low as 1 part in 10^{11}). The high output power and/or the narrow linewidth are specific features that make such sensitivity possible.

Quantum-Optical Properties

S0065

P0340 The pairwise production of signal and idler photons is at the heart of the parametric process. This perfect quantum correlation is to a certain extent also maintained in the output waves of a cwOPO. In particular, the intensity fluctuations of signal and idler waves emitted by a DRO are strongly (albeit never perfectly) quantum correlated if their output coupler transmissions significantly exceed their respective roundtrip losses. For these 'twin beams' the spectral density of the fluctuations of their power difference can be less than the spectral density of the fluctuations of the power of an individual wave (squeezing). Making use of this correlation permits to increase the obtainable sensitivity in spectroscopic measurements for a given power level of the wave interacting with the sample.

Device Development Trends

S0070

P0345 CwOPOs using solid-state pump lasers have become commercially available. In the near future, some likely developments will be miniaturization and optimization in order to reduce the influence of perturbations, further extension of continuous and mode-hop tuning ranges and the wider use of diode lasers as pump lasers, leading to cost reduction.

To access a larger range of molecules in spectroscopy, extension of the emission range well beyond 5 μm is also of significant interest. Novel nonlinear materials and pump lasers of wavelength longer than the often employed Nd:YAG lasers will become of importance in this development.

P0350 Two specific lines of development complementary to the bulk cwOPOs described above are waveguide and intracavity cwOPOs (ICSRO). If pump, signal and idler waves are confined in a waveguide (*see* **Photonic Crystals:** Photonic Crystal Lasers, Cavities and Waveguides (00929)) the parametric gain coefficient is a few orders higher than for free-space Gaussian waves, due to the small mode cross-section and the scaling with the square of the crystal length, compared with the linear scaling in case of Gaussian beams (see eqns [6] and [8]). Values are on the order of $E \sim 1/\mathrm{W}$ at $\lambda_p = 1.5$ μm leading to low thresholds even for SROs, with pump lasers of comparatively long wavelength. For example, in a SRO consisting of a 9 cm long Titanium:PPLN waveguide, a threshold below 300 mW for a 1.5 μm pump was achieved. The idler emission range was 3.1–3.4 μm. The potential for mass production and, therefore, cost minimization is clear.

P0355 An ICSRO consists of an SRO internal to the cavity of a cw laser, where the high circulating laser power is taken advantage of for pumping. An ICSRO is thus similar to a PR-SRO but there is no need to implement a control system for the frequency lock between pump laser and pump cavity nor to mode-match the pump wave to the SRO cavity mode.

Appendix A

S0075 ## Three-Wave Mixing in a $\chi^{(2)}$ Medium with Focused Waves

P0360 The wave equation in a nonlinear medium reads

$$\Delta\vec{E} - \mu_0\mu_r\frac{\partial^2}{\partial t^2}\vec{D}_\mathrm{L} = \mu_0\mu_r\frac{\partial^2}{\partial t^2}\vec{P}_\mathrm{NL} \qquad [8]$$

The displacement field $\vec{D}_\mathrm{L}$ is related to the electric field $\vec{E}$ by linear response. $\vec{P}_\mathrm{NL}$ is the nonlinear polarization. We deal with nonmagnetic media ($\mu_r = 1$) and choose the principal axis system as coordinate system. The Fourier transform of, for example, the x-component of the wave equation then reads:

$$\Delta E_x(\omega,\vec{r}) + \mu_0\omega^2\varepsilon_0\varepsilon_x(\omega)E_x(\omega,\vec{r}) = -\mu_0\omega^2 P_{\mathrm{NL},x}(\omega,\vec{r}) \qquad [9]$$

P0365 In the following, we take into account only second-order nonlinear effects, so the nonlinear polarization reduces to $P_\mathrm{NL} = P^{(2)}$. The fields to be considered are monochromatic, propagate in the z-direction and are linearly polarized along x. The notation can then be simplified to:

$$E_x(\omega,\vec{r}) = \varepsilon(\vec{r})\mathrm{e}^{\mathrm{i}kz}, \quad P_{\mathrm{NL},x}(\omega,\vec{r}) = P^{(2)}_\omega(\vec{r}) \qquad [10]$$

with the wavevector $k = \omega n(\omega)/c$ and the refractive index for the polarization under consideration $n_\omega^2 = n(\omega)^2 = \varepsilon_x(\omega)$. The electric field is obtained as $\vec{E}(t,\vec{r}) = \frac{1}{2}\mathrm{Re}(\varepsilon(\vec{r})\mathrm{e}^{\mathrm{i}(kz-\omega t)})\hat{x}$.

P0370 Since the parametric gains are small in cw conversion, the derivative of the envelope $\varepsilon(\vec{r})$ changes only little over a propagation distance on the order of a wavelength $2\pi/k$. Inserting eqn [9] into eqns [6] and [8] and neglecting the term $\sim \mathrm{d}^2\varepsilon(\vec{r})/\mathrm{d}z^2$, yields the paraxial or slowly varying envelope wave equation:

$$\left(\frac{\partial^2}{\partial x^2} + \frac{\partial^2}{\partial y^2} + 2ik\frac{\partial}{\partial z}\right)\varepsilon = -\mu_0\omega^2 P^{(2)}_\omega(\vec{r})\mathrm{e}^{-\mathrm{i}kz} \qquad [11]$$

The electric field envelope can be expanded in a complete set of Gaussian TEM_{mn} – mode functions ψ_{mn}:

$$\varepsilon(\vec{r}) = \sqrt{\frac{\omega}{n_\omega}}\sum_{m,n=0}^{\infty} A_{mn}(z)\psi_{mn}(\vec{r}) \qquad [12]$$

These mode functions are defined to satisfy the paraxial wave equation in absence of nonlinearity (vanishing right hand side in eqn [11]) and the orthonormality properties

$$\int\int_{-\infty}^{-\infty}\psi^*_{mn}(\vec{r})\psi_{m'n'}(\vec{r})\mathrm{d}x\,\mathrm{d}y = \delta_{mm'}\delta_{nn'} \qquad [13]$$ Q2

P0375 A particular mode function set is characterized by position (along z) and size of the waist, which can be chosen arbitrarily. The functions $A_{mn}(z)$ are slowly varying amplitude functions. The power in a particular mode can be calculated from:

$$P_{mn}(z) = \frac{\omega|A_{mn}(z)|^2}{2\mu_0 c} \qquad [14]$$

where c is the speed of light *in vacuo*. Inserting eqn [12] into eqn [11], multiplication with $\Psi^*_{m'n'}(\vec{r})$, and integration over x, y yields:

$$\frac{\mathrm{d}A_{m'n'}(z)}{\mathrm{d}z} = \mathrm{i}\frac{\mu_0 c}{2}\sqrt{\frac{\omega}{n_\omega}}\mathrm{e}^{-\mathrm{i}kz}\int\int_{-\infty}^{\infty}P^{(2)}_\omega(\vec{r})\Psi^*_{m'n'}(\vec{r})\mathrm{d}x\,\mathrm{d}y \qquad [15]$$

If all electric fields are linearly polarized, the Fourier amplitudes of the nonlinear polarization can be

written as:

$$P^{(2)}_{\omega_s}(\vec{r}) = 2\varepsilon_0 d(z) E_{\omega_p}(\vec{r}) E^*_{\omega_i}(\vec{r})$$
$$P^{(2)}_{\omega_i}(\vec{r}) = 2\varepsilon_0 d(z) E_{\omega_p}(\vec{r}) E^*_{\omega_s}(\vec{r}) \qquad [16]$$
$$P^{(2)}_{\omega_p}(\vec{r}) = 2\varepsilon_0 d(z) E_{\omega_s}(\vec{r}) E_{\omega_i}(\vec{r})$$

where d is the tensor element appropriate to the particular combination of linear polarizations of the three waves. (In eqn [16], $\omega_i + \omega_s = \omega_p$).

The mode amplitude equations for the three interacting waves follow from eqns [10], [15], and [16] as:

$$\frac{\mathrm{d}A^{\{p,s,i\}}_{mn}(z)}{\mathrm{d}z} = \mathrm{i}\frac{d(z)}{c}\begin{Bmatrix}\sqrt{\omega_p/n_p}\,\mathrm{e}^{-\mathrm{i}\Delta kz}\\ \sqrt{\omega_s/n_s}\,\mathrm{e}^{+\mathrm{i}\Delta kz}\\ \sqrt{\omega_i/n_i}\,\mathrm{e}^{+\mathrm{i}\Delta kz}\end{Bmatrix}\int\int \mathrm{d}x\,\mathrm{d}y \times\begin{Bmatrix}\varepsilon_s(\vec{r})\varepsilon_i(\vec{r})\\ \varepsilon_p(\vec{r})\varepsilon_i(\vec{r})^*\\ \varepsilon_p(\vec{r})\varepsilon_s(\vec{r})^*\end{Bmatrix}\psi^{\{p,s,i\}}_{mn}(\vec{r})^* \qquad [17]$$

The quantity $\Delta k = k_p - k_s - k_i$ is the wavevector mismatch. Here, the envelope of each wave has an expansion of the form in eqn [12] with its respective (independent) set of mode functions.

Appendix B

S0080

Steady-State Description of the cwOPO

P0380 The general eqns [17] are applicable to any type of cwOPO. Below and at threshold at least two of the three waves have given modes, i.e., the corresponding function $\varepsilon(\vec{r})$ is known up to a slowly z-dependent amplitude. The resonant parametric wave has a mode defined by the cavity geometry and mirrors, while the pump wave mode is defined by the used focusing optics. This knowledge allows to obtain an analytic expression for the threshold of any OPO type and for an arbitrary cavity. Above threshold two cases can be distinguished:

P0385 (i) in a basic SRO the pump mode itself becomes a function of pump power, due to its depletion by signal and idler wave, and only a numerical solution can be given; and

P0390 (ii) if two or more waves resonate in one or more cavities (DRO, PR-SRO, TRO), an analytic solution is possible even above threshold.

In the following, the PR-SRO is treated. Figure 4 shows a schematic of a common cavity PR-SRO and the notation; the treatment below also holds for the dual cavity PR-SRO. Without loss of generality, the signal wave is taken to be the signal. For the sake of simplicity, below a further assumption about the spatial mode of the idler will be made. P0395

The pump and signal waves are given by TEM_{00} modes of the cavity (or cavities): P0400

$$\varepsilon_p(\vec{r}) = \sqrt{\frac{\omega_p}{n_p}}A_{00p}(z)\psi_{00p}(\vec{r})$$
$$\varepsilon_s(\vec{r}) = \sqrt{\frac{\omega_s}{n_l}}A_{00s}(z)\psi_{00s}(\vec{r}) \qquad [18]$$

In the case of a common-cavity PR-SRO, pump and signal resonate in the same cavity and therefore their modes have the same waist position and Rayleigh ranges $z_R = kw^2/2$, (w is the waist). In the case of a dual-cavity PR-SRO the modes are in principle independent.

Although the idler wave is in general not purely TEM_{00}, it may approximately by a TEM_{00} mode, whose mode parameters are determined by an optimization criterium. We can then introduce the overlap function: P0405

$$O(z) = \int\int \mathrm{d}x\,\mathrm{d}y(\psi_{00p}(\vec{r}))^*\psi_{00s}(\vec{r})\psi_{00i}(\vec{r}) \qquad [19]$$

Under these assumptions, the infinite set of mode eqns [17] reduces to just three coupled equations ($A \equiv A_{00}$):

$$\frac{\mathrm{d}A_p(z)}{\mathrm{d}z} = -\mathrm{i}\xi(z)A_s(z)A_i(z)\mathrm{e}^{-\mathrm{i}\Delta kz}O(z) \qquad [20]$$

$$\frac{\mathrm{d}A_s(z)}{\mathrm{d}z} = -\mathrm{i}\xi(z)A_p(z)A^*_i(z)\mathrm{e}^{\mathrm{i}\Delta kz}O(z)^* \qquad [21]$$

$$\frac{\mathrm{d}A_i(z)}{\mathrm{d}z} = -\mathrm{i}\xi(z)A_p(z)A^*_s(z)\mathrm{e}^{\mathrm{i}\Delta kz}O(z)^* \qquad [22]$$

where

$$\xi(z) = \frac{\mathrm{d}(z)}{c}\sqrt{\frac{\omega_p\omega_s\omega_i}{n_p n_s n_i}} \qquad [23]$$

Two phasematching cases have to be considered: for birefringent phasematching, $d = \mathrm{const}$ and ξ is independent of z. In QPM, the d-coefficient is modulated periodically along z with period Λ. It suffices to consider only the particular term of its Fourier series expansion that gives the smallest wavevector quasi-mismatch. When only the first

term is relevant, this is referred to as first-order QPM and $d(z) \simeq \frac{1}{2}\hat{d}(g_1\, e^{i2\pi z/\Lambda} + \text{c.c.})$. This case can be taken into account by replacing $d(z)$ in eqn [23] by $d_{\text{eff}} = \frac{1}{2}\hat{d}g_1$, and in eqns [20]–[22] the relevant wavevector mismatch becomes $\Delta k = k_p - k_s - k_i \pm 2\pi/\Lambda$, where, for usual materials, the minus sign applies.

P0410 We solve eqns [20]–[22] in the nonlinearity ξ. This is appropriate due to the small gain and implies that the resonant pump and signal wave amplitudes do not change substantially (relative to the respective average amplitude) along the crystal length and around the cavity.

P0415 Integrating eqn [22] after approximating the right-hand side by its value at $z = 0$ yields:

$$\begin{aligned} A_i(z) &= -i\xi z A_p(0) A_s^*(0) I^*(z) \\ I(z) &= \frac{1}{z}\int_0^z dz' O(z') e^{-i\Delta k z'} \end{aligned} \qquad [24]$$

We insert this result into eqns [20] and [21] and approximate $A_s(z)$ and $A_p(z)$ by their values at $z = 0$. The result is

$$A_p(z) = A_p(0) - \frac{1}{2}(\xi z)^2 D^*(z) A_p(0) |A_s(0)|^2 \qquad [25]$$

$$A_s(z) = A_s(0) + \frac{1}{2}(\xi z)^2 D(z) A_s(0) |A_p(0)|^2 \qquad [26]$$

$$D(z) = \frac{2}{z^2}\int_0^z dz' z' I(z') O(z')^*\, e^{i\Delta k z'} \qquad [27]$$

This completes the calculation of the propagation through the nonlinear medium. Now we proceed to calculate the propagation around the cavity.

P0420 Since the signal wave is resonant with the cavity, we can immediately write the self-consistency equation for the roundtrip:

$$|A_s(0)| = \sqrt{R_s(1 - V_s)}\,|A_s(L)| \qquad [28]$$

The roundtrip cavity reflectivity and roundtrip loss for the signal wave are denoted by R_s and V_s. At the input mirror (see lower part of **Figure 4**), characterized by a transmission $T_p = 1 - R_p$, the interference of the injected pump wave $A_{p,in}$ and the internally circulating pump wave must be considered:

$$A_p(0) = \sqrt{T_p} A_{p,in} + \sqrt{R_p(1 - V_p)} A_p(L) e^{i\phi} \qquad [29]$$

V_p is the pump roundtrip loss. Evaluating eqn [24] at $z = L$ and comparing with eqn [25] yields:

$$|A_p(0)|^2 = \left[\frac{1}{\sqrt{R_s(1 - V_s)}} - 1\right] \frac{1}{\frac{1}{2}(\xi L)^2 \text{Re}\, D(L)} \qquad [30]$$

Here the imaginary part of $D(z)$ was neglected since $|\xi L A_p(0)|^2 \ll 1$. Expression [30] shows that the intracavity pump power is clamped at a fixed value, equal to the value at threshold, independent of the input power.

In eqn [29] we can assume $A_{p,in}$ to be real without P0425 loss of generality, yielding the relation:

$$\sqrt{T_p}\frac{A_{p,in}}{A_p(0)} = 1 - \sqrt{R_p(1 - V_p)} e^{i\phi} \frac{A_p(L)}{A_p(0)} \qquad [31]$$

where $\phi = \omega_p \text{OPL}(\omega_p, T)/c$. The pump wave is assumed to be exactly resonant; this means that $A_p(0)$ is maximum. The phase ϕ must therefore be such that:

$$e^{i\phi}\frac{A_p(L)}{|A_p(0)|} \in \mathbb{R} \qquad [32]$$

Together, with eqn [25], we obtain:

$$\left|\frac{A_p(L)}{A_p(0)}\right|^2 = \left|1 - \frac{1}{2}(\xi L)^2 D^*(L) |A_s(0)|^2\right|^2 \qquad [33]$$

The right-hand side is evaluated neglecting the contribution proportional to ξ^4; inserting the result in eqns [31] and [32] gives:

$$\begin{aligned} \sqrt{T_p}\frac{A_{p,in}}{|A_p(0)|} &= 1 - \sqrt{R_p(1 - V_p)} \\ &\quad + \sqrt{R_p(1 - V_p)}\frac{1}{2}(\xi L)^2 \text{Re}\, D |A_s(0)|^2 \end{aligned} \qquad [34]$$

Equations [30] and [34] represent the steady-state solution of the PR-SRO: they give the circulating pump and signal powers, from which all desired quantities can be computed.

The external threshold is found by setting $A_1(0) = 0$ P0430 and assuming small losses, T_p, $V_p \ll 1$

$$P_{p,in}^{th} \simeq \frac{T_p + V_p}{T_p} \cdot (T_p + V_p) \cdot \frac{(T_s + V_s)}{E} \qquad [35]$$

with the nonlinearity

$$E = \frac{2\mu_0 d^2}{\pi c^2}\frac{\omega_s \omega_i}{n_p n_s n_i} L^2\, \text{Re}\, D(L) \qquad [36]$$

Note that $\text{Re}\, D(L) = |I(L)|^2$. The second factor in eqn [35] is responsible for the reduction of threshold due to pump resonance. The last factor is the internal pump threshold and constant circulating pump power level:

$$P_p(0) \simeq \frac{(T_s + V_s)}{E} \qquad [37]$$

which is also equal to the threshold of a basic SRO. The nonlinearity may be written as

$$E \simeq \frac{4\mu_0 d^2}{\pi c^2} \frac{\omega_s^2 \omega_i^2}{n_p^2 \omega_p} L h_{PA} \qquad [38]$$

with the dimensionless focusing function h_{PA}. A detailed calculation shows that the value of h_{PA} cannot exceed 1.1 and is close to its maximum when the phase mismatch ΔkL is approximately zero and the pump and signal focusing by the cavity is such that their Rayleigh range $z_R \simeq L/2$.

P0435 The OPO will select the signal cavity mode frequency ω_s and idler spatial mode that minimizes the threshold eqn [35]. Note that this is not necessarily equivalent to a maximization of E, since T_s and V_s may also be dependent on signal frequency, for example, because of the presence of an etalon inside the cavity.

P0440 The circulating signal power as derived from eqns [30] and [34], is given in eqn [6] and [8].

P0445 The signal power extracted from the cavity is $P_{s,out} = T_s P_s(L) \simeq T_s P_s(0)$, while the (fully extracted) idler power is given by:

$$P_{i,out} = P_i(L) = \frac{\omega_i}{\omega_s} E P_s(0) P_p(0) \qquad [39]$$

See also

S0085

P0450 **Nonlinear Optics, Applications:** Phase Matching (00767). **Optical Parametric Devices:** Overview (00757). (00768).

Further Reading

Applied Physics *B* 66(6): (1998). Q3

Breitenbach G, Schiller S and Mlynek J (1995) *Journal of the Optical Society of America B* 12: 2095–2101. Q4

Drühl K (1998) *Applied Physics B* 66: 677–683.

Ebrahimzadeh M and Dunn MH (2000) Optical parametric oscillators. In: Bass M, Enoch JM, van Stryland EW and Wolfe WL (eds) *Handbook of Optics IV*, pp. 2201–2272. McGraw-Hill. Q5

Ebrahimzadeh M, Turnbull GA, Edwards TJ, Stothard DJM, Lindsay ID and Dunn MH (1999) *Journal of the Optical Society of America B* 16: 1499–1511. Q4

Guha S (1998) *Applied Physics B* 66: 663–675. Q4

Schiller S, Schneider K and Mlynek J (1999) *Journal of the Optical Society of America B* 16: 1512–1524. Q4

Schreiber G, Hofmann D and Grundkötter W, *et al.* (2001) *Proceeding SPIE* 4277: 144. Q4

Yariv A and Yeh P (2002) *Optical Waves in Crystals*. Wiley-Interscience. Q5